
“Nematic Ordered Cellulose”: A Concept of Glucan Chain Association

Tetsuo Kondo, Eiji Togawa, and R. Malcolm Brown, Jr.

Forestry and Forest Products Research Institute (FFPRI),
P.O. Box 16, Tsukuba Norin, Ibaraki 305-8687, Japan; and School of
Biological Sciences, Section of Molecular Genetics and Microbiology,
The University of Texas at Austin, Austin, Texas 78712

*Bio***MACROMOLECULES**

Reprinted from
Volume 2, Number 4, Pages 1324–1330

“Nematic Ordered Cellulose”: A Concept of Glucan Chain Association

Tetsuo Kondo,*[†] Eiji Togawa,[†] and R. Malcolm Brown, Jr.[‡]

Forestry and Forest Products Research Institute (FFPRI), P.O. Box 16, Tsukuba Norin, Ibaraki 305-8687, Japan; and School of Biological Sciences, Section of Molecular Genetics and Microbiology, The University of Texas at Austin, Austin, Texas 78712

Received August 15, 2001

Native cellulose consists of a set of parallel chains composed of glucose. Most of the time, these chains are highly ordered and form a structure that is known as a microfibril. On the other hand, highly crystalline forms of cellulose are more difficult to process and often are unpredictable in their behavior. If an ordered but noncrystalline form of cellulose could be produced, this would greatly extend the possibilities of usage of cellulose to new areas. In this paper, we have produced such a new supermolecular structure of cellulose, called *nematic ordered cellulose*. The unique characteristics of this supermolecular structure of cellulose have been clarified using various kinds of physicochemical analyses. Using a high-resolution transmission electron microscopic approach, we have also imaged the single glucan chains, demonstrating the close but nonprecise association usually found in crystalline biopolymers.

Introduction

Cellulose comprises the major polymer of plant cell walls and has had a long history as a natural polymer material. The biomacromolecule, which is a β -1,4-linked glucan homopolymer, normally is classified according to how the β -glucan chains associate. We expand the concept how various states of molecular association can be categorized in cellulose. A major consideration is that the predominant crystalline state of cellulose is included as a component in the ordered state. This means that the ordered state also contains noncrystalline ordered states. The category “ordered” is in contrast to the “nonordered” state which to date has been considered as “amorphous cellulose” for lack of a useful way to characterize the product. It should be noted that in our concept, the amorphous state being categorized as the “nonordered” state, should be distinguished from the “noncrystalline” state of cellulose. Thus, in this classification, it becomes crucial whether the state is “ordered” or “nonordered”.

Historically, it has been difficult to find an appropriate method to characterize noncrystalline or amorphous domains of cellulose. Often, wide-angle X-ray diffraction (WAXD) has been used for determining the crystalline forms and the crystallinity: however, in most cases when WAXD provides a diffuse diffraction pattern, it is considered simply as “amorphous cellulose”.¹ Thus, we have attempted to determine the “noncrystalline regions” of noncrystalline cellulose films using FT-IR monitoring of the deuterated hydroxyl groups.² We have found that such noncrystalline regions may

comprise at least three different domains. The study² also indicated the presence of ordered domains in the noncrystalline regions. We also reported such an ordered region in primary walls of higher plants which had been thought as amorphous.^{3,4} In fact, the possibility has been discussed that there may be “paracrystalline domains” which may exhibit a certain order in cellulose microfibrils of plant cell walls.⁵

Recently, we developed a new method to obtain a cellulose film which exhibits noncrystalline yet ordered states created by induction of a specific drawing stress from a highly water-swollen cellulose.⁶ This system implies the possibility of changes in states of β -glucan chain association. In this article, we characterize the novel structural arrangements leading to the proposal of a new, ordered, supermolecular structure of cellulose but one which is noncrystalline. We have termed this form of cellulose as “nematic ordered cellulose” (NOC), because the definition of nematic order is well defined for our cellulose supermolecular structure. The nematic phases possess no long range orientational order and produce only diffuse scattering in X-ray diffraction patterns. In this case, the direction of the molecules (“director”) tend to be parallel. The quality of the alignment is not perfect, and is quantified by the order parameter. The basic concept for nematic order was invented by G. Friedel. It comes from Greek $\nu\eta\mu\alpha$ = thread, and refers to certain threadlike defects that are commonly observed in these materials.

Experimental Section

Materials. Bleached cotton linters with a degree of polymerization (DP) of 1300 were used as the starting cellulose sample. The cellulose was first dried under vacuum at 40 °C. *N,N*-Dimethylacetamide (DMAc) purchased from Katayama Chemicals Co. Ltd. (99+%) was dehydrated with

* To whom correspondence should be addressed. E-mail: kondot@ffpri.affrc.go.jp.

[†] Forestry and Forest Products Research Institute (FFPRI).

[‡] The University of Texas at Austin.

molecular sieve 3A and used without further purification. Lithium chloride (LiCl) powder (Katayama Chemicals Co. Ltd.) was oven-dried at least for 3 days at 105 °C.

Sample Preparation. (i) Water-Swollen Cellulose Film from the DMAc/LiCl Solution.⁶ LiCl dried at 105 °C was dissolved in anhydrous DMAc to give a concentration of 5% (w/w) solution. Dissolution of cellulose was basically followed by a previous swelling procedure⁶ using a solvent exchange technique.⁷ Prior to swelling, the cellulose sample was disintegrated into fragments or small pieces by a mechanical disintegrator and dispersed into water, which increased the surface area making it easier to dissolve. The treated cellulose was soaked in water overnight and then squeezed and filtered to remove the water. The cellulose was then immersed in methanol and again squeezed and filtered to remove excess methanol. After four repetitions of the methanol treatments, an exchange with acetone was performed once. Following the treatments with water, methanol, and acetone described above, the sample was solvent-exchanged with DMAc twice in the same procedure and soaked in the same solvent overnight. Another two repetitions of the above soaking and squeezing treatments with DMAc treatments were performed on the sample. Following the final squeeze, the cellulose was ready to be dissolved. The cellulose swollen by DMAc was dissolved in the DMAc/LiCl solution with constant stirring at room temperature for three weeks at most. As the viscosity of the solution depends on the DP of the polymer, ca. 1% cellulose with a DP of 1300 was suitable for handling. After a week, when no change in viscosity was noted in the solution, 1–3% LiCl was added to the solution, and then it was heated to 50–60 °C for several hours. The resulting solution was then centrifuged and filtered to remove any insoluble portion. The actual concentration (wt %) of cellulose in the solution was determined by weighing a small portion of the dried cellulose film. At this stage, the molecules are almost completely dispersed.⁸

The slow coagulation to prepare the gellike film from a DMAc/LiCl solution was carried out according to previous techniques^{6,13} with the following modifications. The solution was poured into a surface-cleaned glass Petri dish with a flat bottom and placed in a closed box containing saturated water vapor at room temperature. In this manner, saturated water vapor slowly diffused into the solution and precipitated the cellulose. The sample was allowed to stand at room temperature for several days until the precipitation under a saturated water vapor atmosphere was sufficiently complete to obtain the gellike film. The precipitated gellike film was washed with running distilled water for several days to remove the solvent, and a water-swollen transparent gellike film was obtained. The films were stored in water until needed. It should be also noted that in the entire procedure from preparation of the solution until starting the slow coagulation with water vapor, rapid operation was required, otherwise the water vapor in the atmosphere would easily penetrate into the solution and cause precipitation of cellulose II crystals.

(ii) Preparation of Drawn Cellulose Films from Water-Swollen Cellulose Films. Drawn cellulose films were

prepared by stretching water-swollen gellike films. These films were cut into strips approximately 30 mm long and 5 mm wide. These water-swollen strips then were clamped in a manual stretching device and elongated uniaxially to a draw ratio of 2.0 at room temperature. As the water-swollen films were gellike, they could neither be clamped too tightly nor too loosely in the first stage of stretching. The entire drawing process was completed while the specimen was still in a wet state. Following air-drying, the drawn specimen in the stretching device was vacuum-dried at 40–50 °C for more than 24 h. The thickness of the dried films for X-ray and CP/MAS ¹³C NMR measurements was about 80 μm.

Measurements. (i) X-ray Diffraction. X-ray diffraction measurements were basically performed according to our previous report.⁶ Wide-angle X-ray diffraction (WAXD) photographs were taken on flat film using nickel-filtered CuK α radiation produced by a Rigaku RINT-2500HF X-ray generator at 40 kV and 40 mA. The WAXD intensity curves with a scanning speed of 0.5°/min were measured by a transmission method using a scintillation counter at 40 kV and 200 mA through the angular range 2θ for the equatorial and the meridional scan to the drawing direction; $2\theta = 5$ –35 and 10–80°, respectively. Instrumental broadening was corrected using Si powder as a standard. The crystallinity from the WAXD intensity curve was calculated assuming that the area ratio was given by the crystalline region area divided by the total area. To avoid complications due to contributions from the sample orientation in this measurement, the sample was cut into small pieces (a coarse powder) that were placed in a 1 mm glass capillary tube. The crystallite orientation parameter, π , for drawn films was estimated followed by the previous method.⁶

(ii) Fourier Transform Infrared (FT-IR) Spectroscopy. FT-IR spectra were obtained using a Perkin-Elmer Spectrum 2000 spectrometer system equipped with a polarizer. Thirty-two scans were averaged with a resolution of 2 cm⁻¹. IR spectra of the crystalline and noncrystalline regions for drawn specimens were measured before and after deuteration with D₂O vapor according to the previous method.^{2,6}

(iii) CP/MAS ¹³C NMR Spectroscopy. The NMR spectrometer used was a Chemagnetics CMX-300 operating at resonance frequencies of 75.57 MHz for ¹³C. ¹³C NMR spectra with cross polarization/magic angle spinning (CP/MAS) were obtained at room temperature. Cross polarization times typically were 1–2 ms. The recycle time of the pulse sequence was 10 s. The spectra were accumulated ca. 500 times. The chemical shift (29.47 ppm from (CH₃)₄Si) of the CH for adamantane crystals was used as an external reference to determine chemical shifts.

(iv) Atomic Force Microscopy (AFM). AFM images of the cellulose film specimens were acquired on a Nanoscope IIIa (Digital Instruments) microscope. AFM was performed at room temperature, being controlled in contact (DC) mode with a scan rate from 1 to 3 Hz to observe 5 × 5 μm² areas. The AFM tip employed was an etched-silicon AFM tip, with a nominal radius from 5 to 15 nm, a cone angle of 35 deg, and a height of about 15 μm, which was mounted on a rectangular type cantilever with a spring constant of 0.13 N m⁻¹. The scanning was carried out in both directions of the

stretching axis of the film and perpendicular to the axis. The width and height of the aggregates were measured using a cross-sectional line profile analysis. Since the width data included geometrical enhancement due to the tip radius, they can be corrected using an equation introduced previously.^{4,10} In our case, as the height of the aggregates was smaller than radius of the tip, the following correction equation was employed:

$$E = 2(RH - H^2)^{1/2}, \quad w = W - E$$

Here, E = geometrical enhancement on the real width value (w), W = apparent width observed in AFM, H = height of the object observed in AFM, and R = the AFM tip radius.

In this study, we employed the R value as 10 nm in radius.

(v) High Resolution Transmission Electron Microscopy (HRTEM). For sample specimens examined by high-resolution transmission electron microscopy, the cellulose solutions were also prepared in the same way as described above and diluted 100 times with water-free DMAc (1.0×10^{-2} wt %). After the solution covered a 3.0 mm TEM grid coated with a Formvar film, the grid was left for more than 3 days at room temperature under a saturated water vapor. During this period, a cellulose gellike film was precipitated and at the same time was naturally stretched across the 3.0 mm diameter of the TEM grid. It was then washed thoroughly with distilled water to exchange the solvent prior to the addition of the negative stain (aqueous 2% uranyl acetate) and finally air-dried. Interaction with uranyl acetate appears to protect samples from electron beam damage.¹¹ Specimens were observed with a Philips EM 420 transmission electron microscope operated at 100 kV with a beam current less than $5 \mu\text{A}$. TEM images were acquired at magnifications of 210K and 450K using a GATAN Model 622 camera. The magnification factor for conversion to the digital image was $23\times$. The images were digitized, saved, and processed by Image Pro Plus software v.4.1 (Media Cybernetics).

Results and Discussion

(i) WAXD and FT-IR Analyses. Water-swollen gellike films formed after slow coagulation and subsequent solvent-exchange were transparent and composed of approximately 93 wt % water and 7 wt % cellulose prior to stretching. When stretching the water-swollen film uniaxially, drops of water extruded from the film as the orientation of the film increased. When the draw ratio reached 2.0, the orientation parameter calculated from WAXD photographs (Figure 1) became 0.88, which indicated a high degree of orientation. However under these conditions, the crystallinity did not significantly follow the increase of the orientation by stretching.⁶ Simultaneous orientation and crystallization did not occur as often seen with crystalline polymers.¹² The crystallinity was ca. 13.8 and 16.3% before and after stretching, respectively. IR spectra of deuterated samples also supported a low crystallinity of the film based on the ratio of the remaining hydroxyl groups in the drawn films which corresponds to the crystallinity index.

Figure 1 shows WAXD intensity curves in both equatorial and meridional directions of the stretched film together with

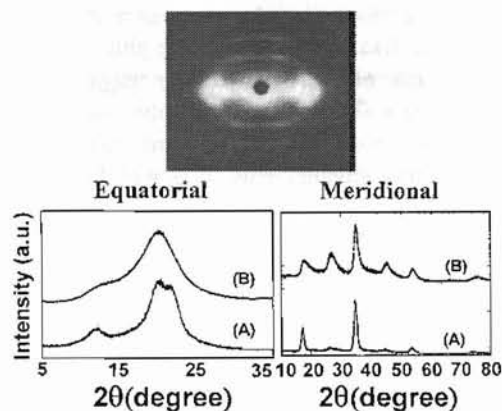


Figure 1. Equatorial (left) and meridional (right) intensity curves of the WAXD for cellulose II fibers (A) and the stretched film studied (B). The term, "a.u." indicates arbitrary unit.

cellulose II fibers. In the equatorial diffraction of the stretched film, crystalline diffraction orders representing cellulose II (Figure 1A) were not observed. The diffuse intensity profile for the stretched film indicated that it contains considerably more "amorphous" regions. The meridional scan of WAXD was employed to analyze the order along the fiber direction for the stretched sample. Meridional intensities of cellulose are affected by the disorder of the neighboring chains which is symmetrical for the chain axis. In general, cellulose polymorphs provide almost the same meridional patterns; namely two strong distinct reflections of the (002) and (004) planes ($2\theta = 17.2^\circ$, $d = 0.516$ nm; $2\theta = 34.7^\circ$, $d = 0.259$ nm, respectively; see the right meridional side of Figure 1A). The present results demonstrate that our highly ordered but noncrystalline stretched cellulose film, gives a totally different profile for the meridional scan as shown in Figure 1B. More reflections were found in the meridional direction when compared with cellulose II crystals. The characteristics are considerable line broadening of the meridional reflections in the profile of the stretched cellulose. This indicates that the structure of the stretched cellulose film along the chain direction may have a certain disorder which causes the ordered, but noncrystalline regions. It may be considered that the situation is not a perfect disorder in the molecular chain direction, but some registrations may exist. Considering the crystallinity of the film sample (16.3%), the meridional direction profile should contain the contribution due to cellulose II crystals. When the contribution of the crystallite is subtracted from the meridional direction profile in Figure 1B, each reflection in the same figure would tend to have the same shape and intensity. Thus, we should consider the states of the structure for the stretched cellulose film to be ordered states that are neither crystalline nor amorphous.

It should be noted that X-ray diffraction patterns showed molecular orientation in the drawn samples, so we wanted to learn if it might be possible to image these oriented glucan chains at the molecular level. Parallel to the X-ray diffraction, the drawn films exhibited a diffuse pattern in the TEM electron diffraction mode, similar to that from X-ray diffraction (not shown here).

(ii) Ordered vs Transitional Order Leading to Crystallization. From cellulose/LiCl/Dimethylacetamide (DMAc) solution remaining overnight under a saturated water vapor,

a gellike film is formed. Film formation may involve a coagulation and fixation process of the glucan chains. This requires formation of hydrogen bonding networks by a slow exchange of the solvent with water molecules. Such slow coagulation, however, may cause a minimum number of hydrogen bonding engagements. It is well-known that the thermodynamically stable crystalline cellulose allomorph, cellulose II, easily is precipitated after a rapid exchange of the organic solvent to liquid water.¹³ On the contrary, once the gellike film is slowly formed under saturated water vapor in our case, a transparent water-swollen gellike film is formed even after washing and exchanging the solvents to liquid water. The preformed hydrogen bonding networks due to water vapor may prohibit the normal molecular stacking required to produce cellulose II crystals. The difference between the normally rapid solvent exchange processes and our slow coagulation basically may be due to the states of water as an exchanging solvent. In liquid water, molecules form clusters, whereas water vapor may be composed of isolated water molecules¹⁴ which could easily diffuse into the solution without solvent-exchange and thus cause hydrogen bonding networks instead of forming cellulose II crystals. This gellike film is considered to exist in either a nonordered state or a liquid crystalline state as reported previously for relatively concentrated LiCl–DMAc cellulose solution.¹⁵ When this wet film is stretched, a highly ordered noncrystalline state forms as a gellike film that can be highly drawable. After the stretched film was dried to be a solid-state film, the order was not changed. In this case, the ordered structure does not necessarily cause crystallization of the polymer because of the presence of the preformed hydrogen bonding networks. A nonordered state has been transformed into an ordered yet noncrystalline state.⁶ We should add that it is hard to judge whether the starting gellike water swollen film may be in either a nonorder or a liquid crystalline state as reported in many cellulose derivatives¹⁶ as well as cellulose.^{7,15} However, our stretched dried film, which is ordered yet noncrystalline, is composed of neither typical lyotropic nor thermotropic liquid crystals, but may be a solid-state ordered film.

(iii) **CP/MAS ¹³C NMR Analyses.** The type of hydroxymethyl conformation at the C-6 position is assumed to provide the extent of crystallization, as well as the final morphology of cellulose.^{6,17} The conformation of C(5)–C(6) and the resulting interactions including hydrogen bonds in the present cellulose structure may differ from that in crystallites. In the noncrystalline regions, the rotational position of hydroxymethyl groups at the C-6 position may be considered as indeterminate or totally nonoriented, whereas all of those are identical in the crystallites. Therefore, it was important to confirm the type of O(6) rotational position with respect to the O(5) and C(4) in a β -glucan chain, employing CP/MAS ¹³C NMR.

CP/MAS ¹³C NMR may suggest the type of hydroxymethyl conformations, *gauche–trans* (*gt*), *trans–gauche* (*tg*), or *gauche–gauche* (*gg*), at the C-6 positions in carbohydrates as shown in Figure 2. Horii et al.¹⁸ indicated that C-6 carbon resonance occurs only as a singlet near 64 ppm in the case of the *gt* conformation whereas a resonance band near 66

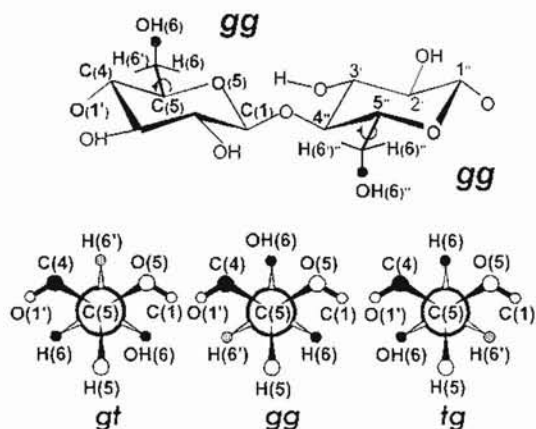


Figure 2. Schematic diagram of the hydroxymethyl conformations at the C-6 position, namely the orientation of the C6–O6 bond, *gauche–trans* (*gt*), *trans–gauche* (*tg*), or *gauche–gauche* (*gg*) with a cellobiose unit.

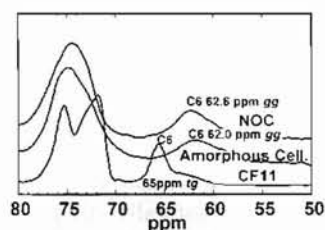


Figure 3. CP/MAS ¹³C NMR spectra of NOC, amorphous cellulose, and native cellulose powder (Whatman CF11).

ppm appears when the *tg* conformation is present within the crystalline structures. According to these researchers, the chemical shifts fall into three groups of 60–62.6, 62.5–64.5, and 65.5–66.5 ppm, which are related to *gg*, *gt*, and *tg* conformations, respectively. The chemical shift of the C-6 for cellulose II^{19–22} indicated the *gt* conformation, which may agree with recent results from the neutron fiber diffraction analysis.²³ As for the noncrystalline states, they are considered in the *gg* conformation. Therefore, it is easy to predict that our stretched cellulose sample could have *gg* conformation of the hydroxymethyl group at the C(6) position.

In Figure 3, the CP/MAS ¹³C NMR spectra for our nematic ordered cellulose (NOC) sample, as well as amorphous (a noncrystalline state without any preferred orientation) cellulose prepared from cellulose–SO₂–dimethylamine–dimethyl sulfoxide solution²⁴ and CF11 cellulose powder (Whatman International Ltd.) are shown in the range from 50 to 80 ppm where chemical shifts at the C(6) position appear. The chemical shift of CF11 appears at 65 ppm, corresponding to *tg* conformation, indicating that CF11 is native cellulose. Our NOC sample exhibits a broader signal similar to amorphous cellulose within the range of the type of the hydroxymethyl conformation, *gg*, which also supports our suggestion that NOC is noncrystalline even though it is well ordered.

(iv) **AFM and HRTEM Analyses.** Using high-resolution microscopic techniques, much effort has been expended to obtain images of the crystalline lattice^{25,26} as well as the crystalline arrangement of cellulose.^{27,28} These images, however, are limited to the microcrystalline regions of cellulose which are very susceptible to damage by the electron beam.

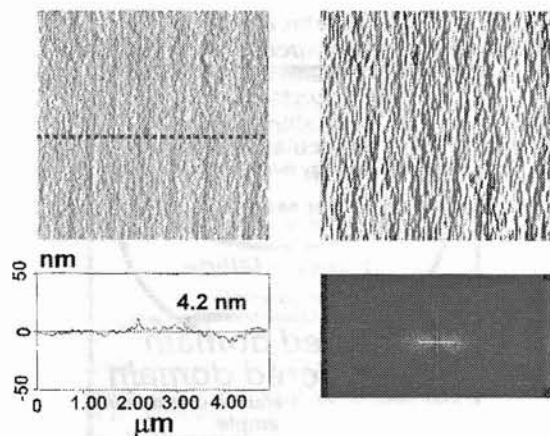


Figure 4. Cross section and the Fourier transformed patterns of AFM images. AFM image of height mode (left) and an inverted enhanced image after Fourier transformation of the original one for a nematic ordered cellulose film (right).

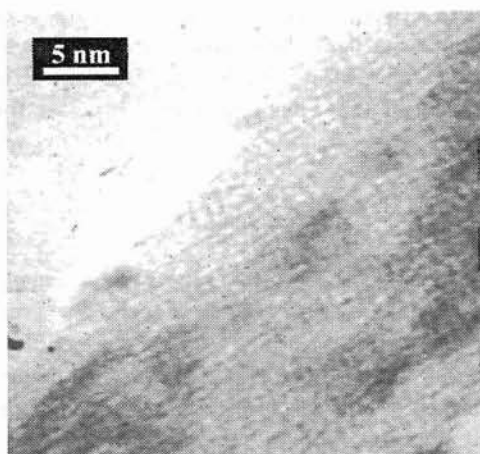


Figure 5. HRTEM image of single β -glucan chains in ordered, noncrystalline regions of the stretched nematic ordered cellulose. The sample on the grid was negatively stained with 2% uranyl acetate. Interaction with uranyl acetate appears to protect samples from electron beam damage. Scale bar indicates 5 nm.

We employed atomic force microscopy (AFM) at different scales to examine the supermolecular structure of our cellulose samples physically produced by the uniaxial drawing of highly water-swollen film states as well as glucan chains. At the resolution on the nanometer scale, AFM images and the cross-section of the surface of the cellulose film shown in Figure 4 demonstrate that well-aligned molecular aggregates with a width of a few nanometers and a height of ca. 4 nm in average are oriented uniaxially.

We used HRTEM to determine the glucan chain associations in our cellulose. Figure 5 shows an image of individual β -glucan chains in this ordered yet noncrystalline cellulose. Even after 10 s of electron beam irradiation, the negatively stained cellulose image was very stable. The glucan chains appear to be decorated with the uranium (induced from uranyl acetate for the negative staining in the sample chamber of TEM), allowing them to be imaged.¹¹ The average chain width of a single, imaged chain was 0.50 nm (the detailed statistical data from Figure 7 will be presented below), corresponding to the dimensions of the space filling model of a single glucan chain viewed from its narrow axis as shown Figure 6. The space filling model allows an accurate prediction of chain dimensions of 0.9–1.0 nm and 0.4–0.5

Cellulose unit in Cellulose structure

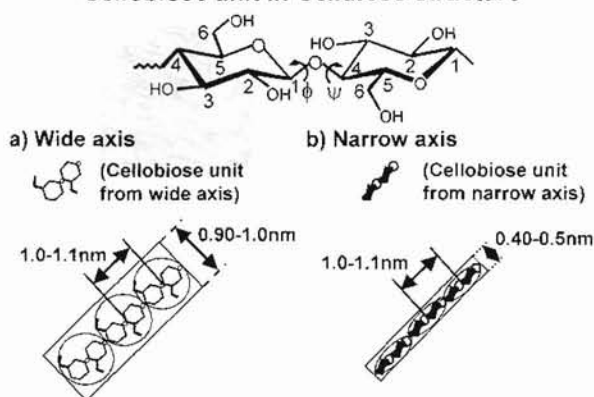


Figure 6. Schematic diagram of a single β -glucan chain viewed from the wide and narrow axes based on standard space filling models.

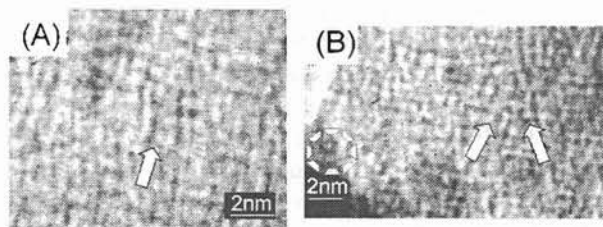


Figure 7. Higher magnification views in the electron micrograph of Figure 5. Note the individual chains are ordered, but they are not crystalline. (A, B). In part B, the 0.24 nm crystalline lattice of uranium is clearly resolved. In both electron micrographs, individual glucan chains are clearly decorated by the uranium. Arrows indicate the predominant molecular directions of the glucan chains. The scale bar indicates 2 nm.

nm from the wide and narrow axes, respectively (Figure 6). Therefore, the TEM image, like the AFM image, clearly exhibited well-ordered, single β -glucan chains in the narrow axis, judging from the average width of a chain.

A higher magnification view (Figure 7) of the same region shown in Figure 5 clearly reveals that the 0.24 nm uranium orthorhombic crystalline lattice is well resolved with a minimum of astigmatism (see the circle in Figure 7B). The crystal lattice constant ($=0.24$ nm) could also be used as an internal reference calibration in addition to graphite ($=0.335$ nm). Other approaches using this HRTEM approach have shown that when the uranyl acetate is exposed to the electron beam, the acetate is removed, leaving elemental uranium which migrates to form the 0.24 nm uranium orthorhombic crystalline lattice.¹¹ As noted above, individual glucan chains were visible largely due to the surface decoration by the negative stain. It should be noted that crystalline cellulose microfibrils do not allow the penetration of uranyl acetate into the lattice.

The HRTEM observations of Figure 7 confirmed the mean width of a single glucan chain corresponding to its known dimensions viewed from its narrow axis of the anhydroglucose ring. The average chain width was 0.462 nm (standard deviation $= \pm 0.0517$ nm). Thus the true width seems to be ca. 0.4–0.5 nm when taking into account the negative stain. The average distance between two parallel chains was 0.660 nm (standard deviation $= \pm 0.068$ nm). Considering that the standard deviations were quite small from over 50 samples measured in each case, the single β -glucan chains in this ordered region are thought to be oriented with the same molecular surface facing the chains, besides taking account

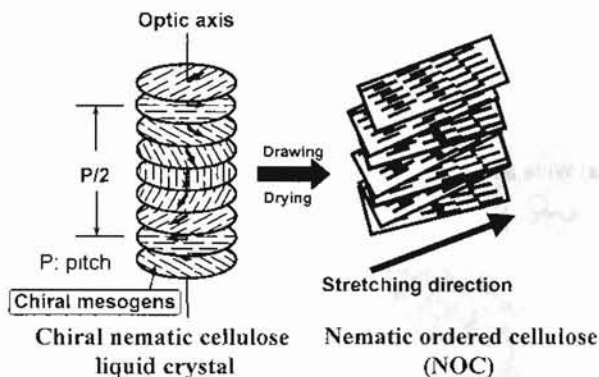


Figure 8. Proposed formation of nematic ordered cellulose (NOC) from chiral nematic cellulose liquid crystals.

of the uranium. In addition, considering that the crystalline lattice plane viewed from its narrow axis of the glucose ring in the regenerated cellulose II crystalline form is (110) with a distance of 0.45 nm between the planes, the well-ordered region is not a regenerated crystalline cellulose II domain. It should be also noted that in another experiment the same region was confirmed to be noncrystalline by a diffuse electron diffraction pattern (not shown). Since the average distance between any two chains in well-ordered states was 0.66 nm, this is wider than the crystal lattice parameters of 0.60 nm between (1 $\bar{1}$ 0) planes, 0.54 nm between (110) planes, and 0.39 nm between (200) planes for native crystalline cellulose I.^{24,25} Therefore, our cellulose has an ordered structure, yet it seems to exhibit no crystalline order.

As shown in the arrow of Figure 7A, we could mostly see the single orientation of the molecular chains, while two orientations appeared sometimes as seen in the two arrows of Figure 7B. This indicates that the present structure may have a layered structure in the depth direction.

(v) A New Supermolecular Structure of Cellulose. The polarization FTIR data (to appear in a following paper) and X-ray results in the previous section of this article confirmed the imaged molecular order of this cellulose. These data suggest that the molecular chain axes have an angular range from 0 to 10 deg to the stretching direction.

To our knowledge, this is a new supermolecular structure of cellulose. Consequently, we have termed this form of cellulose, "nematic ordered cellulose" (NOC), because the definition of nematic order is well defined for our cellulose supermolecular structure in a plane (2D): the nematic phases possess no long-range orientational order, causing only diffuse scattering in the X-ray diffraction pattern; however, in the direction of the molecules ("director") they tend to be parallel. The quality of the alignment is not perfect, and is quantified by the order parameter. For the 3-D structure of NOC, a tentative model (shown in the right of Figure 8) clearly explains the X-ray, FTIR, and CP/MAS ¹³C NMR results as well as the present AFM and TEM observations. This novel cellulose may be considered as a self-ordering structure closely resembling that of a liquid crystal. This is based on the accumulation of nematic layers with an angular range of 0–10 deg to the stretching direction between the layers. In other words, we have postulated this cellulose to be a stretched structure of a chiral nematic mesophase (cholesteric structure) which often is seen in cellulosic liquid

A concept of glucan chain association in cellulose

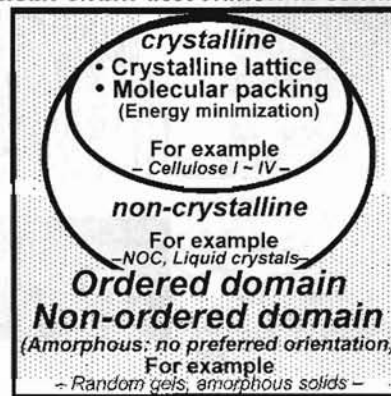


Figure 9. Our concept of glucan chain association for cellulose.

crystals as shown in Figure 8. As described above, Figure 7B shows that two molecular chain orientations were seen, indicating that at least two layers may be crossed or accumulated with respect to each other. This may be indirect evidence favoring the schematic layered structure for NOC in Figure 8.

Conclusion

We wish to emphasize in this report that in categorizing the states of cellulose molecular association, it may be advantageous to first prioritize whether the cellulose is in the ordered or nonordered domain, rather than determine if it is crystalline or noncrystalline. Figure 9 demonstrates the schematic representation of our concept. In this idea, a noncrystalline state in the ordered domain should have intermediates from amorphous to crystalline states, and these are important in determining further states of aggregation which may lead to the crystalline state. Of course, the crystalline states are important, but so far, too much attention has been paid only for crystalline structures. A key concept here is that we should consider crystalline states as a subdivision of the more broad concept of ordered domains. In this concept, "nematic ordered cellulose (NOC)" is considered as an intermediate between the truly crystalline forms of celluloses I–IV and the randomly ordered, noncrystalline (amorphous) phases. These findings create a new concept to understand how β -glucan chains associate and crystallize and also indicate that newly discovered forms may have expanded and useful properties for commercial utilization.

Finally, it should be stated that our concept may be extended to the natural process to explain the degree of glucan chain association which is probably under the control of a multicomponent enzyme complex (TC) that modulates not only the simultaneous polymerization of glucan chains but also how these glucan chains associate to form a metastable crystalline sub-microscopic microfibril with a composite of two sub-allomorphs, I α and I β found in the 1980s by Atalla and VanderHart.²⁹

Acknowledgment. We thank Ms. Y. Hishikawa (FFPRI) and Ms. W. Kasai (The University of Tokyo) and Dr. D.

Romanovicz (The University of Texas at Austin) for their technical assistance of FT-IR, AFM measurements, and preparation of the manuscript, respectively. We also are indebted to Mr. Richard Santos for his assistance with the experiments. This research was in part supported by a Joint Research Program between Japan and US through the Science and Technology Agency of Japan and by the Welch Foundation (F-1217), and the Johnson & Johnson Centennial Chair Funds.

References and Notes

- (1) For example; Klemm, D.; Philipp, B.; Heinze, T.; Heinze, U.; Wagenknecht, W. In *Comprehensive Cellulose Chemistry*. vol.1, Wiley-VCH: Weinheim, Germany, 1998; p 204.
- (2) Hishikawa, Y.; Togawa, E.; Kataoka, Y.; Kondo, T. *Polymer* **1999**, *40*, 7117.
- (3) Kataoka, Y.; Kondo, T. *Macromolecules* **1998**, *31*, 760.
- (4) Kondo, T. In *Advances in Lignocellulosics Characterization*; Argyropoulos, D., Ed.; Tappi Press: Atlanta, GA 1999; Chapter 14, p 337.
- (5) (a) Wardrop, A. B. In *The formation of wood in forest trees*; Zimmermann, M. H., Ed.; Academic Press: New York, 1964; p 87.
(b) Harada, H.; Côté, W.A., Jr. In *Biosynthesis and biodegradation of wood components*; Higuchi, T., Ed., Academic Press: Orlando, FL, 1985; p 1.
- (6) Togawa, E.; Kondo, T. *J. Polym. Sci., B: Polym. Phys.* **1999**, *37*, 451.
- (7) Chanzy, H.; Peguy, A.; Chaunis, S.; Monzic, P. *J. Polym. Sci. Polym. Phys. Ed.* **1980**, *18*, 1137.
- (8) Matsumoto, T.; Tatsumi, D.; Tamai, N.; Takaki, T. *Cellulose* **2001**, in press.
- (9) Ritcey, A. M.; Gray, D. G. *Biopolymers* **1988**, *27*, 1363.
- (10) Kataoka, Y.; Kondo, T. *Planta*, submitted for publication.
- (11) Spires, T.; Brown, R. M. **2001**. In preparation.
- (12) Ward, I. M. In *Structure and Properties of Oriented Polymers*; Ward, I. M., Ed.; Chapman & Hall: London, 1997, p 1.
- (13) For example, Rånby, B. *Cell. Chem. Technol.* **1997**, *31*, 3.
- (14) Tödheide, K. In *Water A comprehensive treatise*; Franks, F., Ed, Plenum Press: New York and London, 1972; Volume 1, The Physics and Physical Chemistry of Water, p 507; Linder, H., Doctoral dissertation, University of Karlsruhe, 1970.
- (15) McCormick, C. L.; Callais, P. L.; Hutchinson, H., Jr. *Macromolecules* **1985**, *18*, 2394.
- (16) Gray, D. G. *J. Appl. Polym. Sci., Appl. Polym. Symp.* **1983**, *37*, 179.
- (17) Kondo, T.; Sawatari, C. *Polymer* **1996**, *37*, 393.
- (18) Horii, F.; Hirai, A.; Kitamaru, R. *Polym. Bull.* **1983**, *10*, 357.
- (19) Dudley, R. L.; Fyfe, C. A.; Stephenson, P. J.; Deslandes, Y.; Hamer, G. K.; Marchessault, R. H. *J. Am. Chem. Soc.* **1983**, *105*, 2469.
- (20) Fyfe, C. A.; Stephenson, P. J.; Veregin, R. P.; Hamer, G. K.; Marchessault, R. H. *Carbohydr. Chem.* **1984**, *3*, 663.
- (21) Isogai, A.; Usuda, M.; Kato, T.; Uryu, T.; Atalla, R. H. *Macromolecules* **1989**, *22*, 3168.
- (22) Horii, F.; Hirai, A.; Kitamaru, R.; Sakurada, I. *Cellulose Chem. Technol.* **1985**, *19*, 513.
- (23) Langan, P.; Nishiyama, Y.; Chanzy, H. *J. Am. Chem. Soc.* **1999**, *121*, 9940.
- (24) Isogai, A.; Atalla, R. H. *J. Polym. Sci., Polym. Chem. Ed.*, **1991**, *29*, 113.
- (25) Sugiyama, J.; Harada, H.; Fujiyoshi, Y.; Uyeda, N. *Mokuzai Gakkaishi* **1985**, *31*, 61.
- (26) Sugiyama, J.; Harada, H.; Fujiyoshi, Y.; Uyeda, N. *Planta* **1985**, *166*, 161.
- (27) Baker, A. A.; Helbert, W.; Sugiyama, J.; Miles, M. J. *J. Struct. Biol.* **1997**, *119*, 129.
- (28) Kataoka, Y.; Kondo, T. **2001** Manuscript in preparation for *Biomacromolecules*.
- (29) Atalla, R. H.; VanderHart, D. L. *Science* **1984**, *223*, 283–285.

BM0101318